

1 Measurement of the $e^+e^- \rightarrow \pi^+\pi^-\pi^0$ cross section in 2 the centre-of-mass range 0.62 to 3.5 GeV at Belle II

3 **Yuki Sue*** on behalf of the Belle II Collaboration

4 *Kobayashi-Maskawa Institute, Nagoya University, Furo-cho, Nagoya, Aichi 381-8602, Japan*

5 *E-mail: ysue@hepl.phys.nagoya-u.ac.jp*

We report a measurement of the $e^+e^- \rightarrow \pi^+\pi^-\pi^0$ cross section in the energy range from 0.62 GeV to 3.5 GeV using an initial-state radiation technique. We use an e^+e^- data sample corresponding to 191 fb^{-1} of integrated luminosity, collected at a centre-of-mass energy at or near the $\Upsilon(4S)$ resonance with the Belle II detector at the SuperKEKB collider. The uncertainty at the ω and ϕ resonances is 2.2%. The leading order hadronic vacuum polarisation contribution to the muon anomalous magnetic moment using this result is $a_\mu^{3\pi} = (48.91 \pm 0.23 \pm 1.07) \times 10^{-10}$. This result differs by 2.5 standard deviations from the current most precise determination.

*42nd International Conference on High Energy Physics (ICHEP2024)
18–24 July 2024
Prague Congress Centre, Prague, Czech Republic*

*Speaker

1. Introduction

The muon anomalous magnetic moment, denoted by $a_\mu \equiv (g - 2)/2$, is one of the physical quantities for which a discrepancy is observed between the experimental and theoretical values. This discrepancy suggests the possibility of a contribution from physics beyond the Standard Model (SM). The experimental value has been determined by the BNL [1] and Fermilab [2, 3] experiments with a precision of less than 200 ppb. The SM prediction reported by the Muon $g - 2$ Theory Initiative [4] disagrees with the experimental values, with a discrepancy exceeding five standard deviations. The theoretical value of a_μ is calculated by summing up the effects of quantum loop corrections in all SM sectors. The QED contribution dominates the value, yet the a_μ uncertainty is dominated by the hadronic vacuum polarisation (HVP) contribution. The HVP contribution is calculated using the measured cross sections for $e^+e^- \rightarrow \text{hadrons}$ processes as the theoretical input. However, recent calculations of the HVP contributions using lattice QCD do not agree with the data-driven values but rather are reported to be closer to the experimental values [5–8]. Furthermore, a new measurement of the $e^+e^- \rightarrow \pi^+\pi^-$ production cross section has been reported from the CMD-3 experiment [9], which deviates significantly from the preceding experiments. Verification with independent experimental setups and data sets is crucial to understanding this complex HVP situation.

To estimate the HVP contribution in the data-driven method, cross sections for $e^+e^- \rightarrow \text{hadrons}$ processes in the exclusive channel at energies below 2 GeV play an essential role. The $e^+e^- \rightarrow \pi^+\pi^-\pi^0$ process is the second largest contribution to the uncertainty on a_μ . The cross sections around the ω and ϕ resonances are particularly important in the contribution, where the systematic uncertainty dominates. In the vicinity of the ω , cross-section differences of up to about 8% have also been observed between the CMD-2 and SND results. The a_μ contribution is estimated with an accuracy of 1.2% based on a global fit to previous experiments.

The Belle II experiment at the SuperKEKB collider [10] at KEK, Japan, aims to measure the light hadron cross sections using e^+e^- collision data operated at or near the e^+e^- centre-of-mass energy of 10.58 GeV. Nevertheless, even in early Belle II analyses, cross sections are expected to be measured with a systematic uncertainty of about 2 percent. Concurrently, this is the first measurement of the $e^+e^- \rightarrow \text{hadrons}$ cross-section in the Belle II experiment, thus providing a reliable benchmark for subsequent measurements of further processes, including $e^+e^- \rightarrow \pi^+\pi^-$, which exhibits the most substantial contribution and uncertainty to the HVP.

2. Analysis overview

The measurement uses an e^+e^- data set with the integrated luminosity of 191 fb^{-1} collected during 2019–2021 in the Belle II detector [11]. To reduce experimenter bias, all actual data is analysed after determining analytical methods and correction factors.

The $e^+e^- \rightarrow \pi^+\pi^-\pi^0$ process with an initial-state radiation (ISR) photon of high energy, typically above 4.7 GeV, is taken as signal events to allow the measurement over a continuous hadronic energy spectrum below 3.5 GeV at the fixed energy e^+e^- collision.

The signal event, $e^+e^- \rightarrow \pi^+\pi^-\pi^0\gamma_{\text{ISR}}$, is reconstructed from two oppositely charged particles and three photons. π^0 is reconstructed from two photons of energy greater than 100 MeV. The ISR

47 photon is selected from photons with energy above 2 GeV and emitted at a large opening angle from
 48 the e^+e^- beam axis. This ISR selection is chosen to satisfy the calorimeter-based trigger condition
 49 and gives an efficiency of more than 99% for ISR-related events. A kinematic fit is imposed on all
 50 $2\pi3\gamma$ candidates found. The fit imposes the constraint that the sums of four-momenta of the final
 51 state coincide with those of the initial e^+e^- . The quality of the kinematic fit χ^2 is sensitive to the
 52 signal topology; the small χ^2 events are selected as signal candidates, while large χ^2 events can
 53 be used to estimate the background level. In addition, several background suppression criteria are
 54 imposed to reduce possible major background events.

55 After all event selection criteria are applied, the events are binned by three-pion invariant mass
 56 $M(3\pi)$. The π^0 signal is extracted by performing a diphoton invariant mass $M(\gamma\gamma)$ on the events
 57 on each $M(3\pi)$ bin. This allows us to exclude background events of photon combinations for which
 58 π^0 is not correctly reconstructed. Residual background processes are mainly $e^+e^- \rightarrow \pi^+\pi^-\pi^0\pi^0\gamma$,
 59 $e^+e^- \rightarrow K^+K^-\pi^0\gamma$ and non-ISR $e^+e^- \rightarrow q\bar{q}$. Background-dominant data control samples are
 60 prepared for each background process. Backgrounds related to final-state radiation are estimated
 61 based on perturbative QCD and previously measured parameters.

62 The obtained $M(3\pi)$ spectrum is distorted, especially near the ω and ϕ resonances, because
 63 the change in cross section is steep compared to the detector resolution. This effect is mitigated
 64 with an iterative-dynamic-stable unfolding method [12].

65 Signal efficiency is estimated with simulated samples of 10 times the data statistics is 7–9%,
 66 depending slightly on $M(3\pi)$. The possible difference in the efficiency between the data and sim-
 67 ulation is divided into several elements and validated with data control samples: trigger efficiency,
 68 ISR photon detection efficiency, tracking efficiency, π^0 reconstruction efficiency, kinematic fit χ^2
 69 selection efficiency, and background suppression efficiency. The background suppression efficiency
 70 causes the largest difference between data and simulation, $(-1.9 \pm 0.2)\%$. The total difference is
 71 $(-4.6 \pm 2.0)\%$ in the energy region below 1.05 GeV. This data-to-simulation difference is used as
 72 a correction factor for the signal efficiency.

73 The total systematic uncertainty for the cross section around the ω and ϕ resonances, where
 74 the systematic uncertainty is dominant, is 2.2%. Of the 2.0% systematic uncertainty for the signal
 75 efficiency correction, the uncertainties for π^0 detection efficiency and tracking efficiency are larger,
 76 at 1.0% and 0.8%, respectively. The integrated luminosity of the data set is measured using the
 77 $e^+e^- \rightarrow e^+e^-$ process, confirmed by the $e^+e^- \rightarrow \gamma\gamma$, and $e^+e^- \rightarrow \mu^+\mu^-$ events, with a systematic
 78 error of 0.63% [13]. In addition, this systematic uncertainty of 1.2% comes from the uncertainty
 79 for the Monte-Carlo generator due to the insufficient data reproducibility of the higher order ISR
 80 photon emission process reported in the BABAR experiment [14].

81 3. Results

82 The measured cross sections are shown separately for each energy range in Fig. 1. The
 83 differences between the other experiments from the fitted values to our result are shown in Fig. 2
 84 in the ω region, where the cross section is large and significantly contributes to the HVP. We
 85 observed the cross sections 5–10% larger than in the other experiments near the resonance peak.
 86 The statistical uncertainty is significant for the mass region above 1.05 GeV but agrees with the
 87 BABAR result rather than the SND.

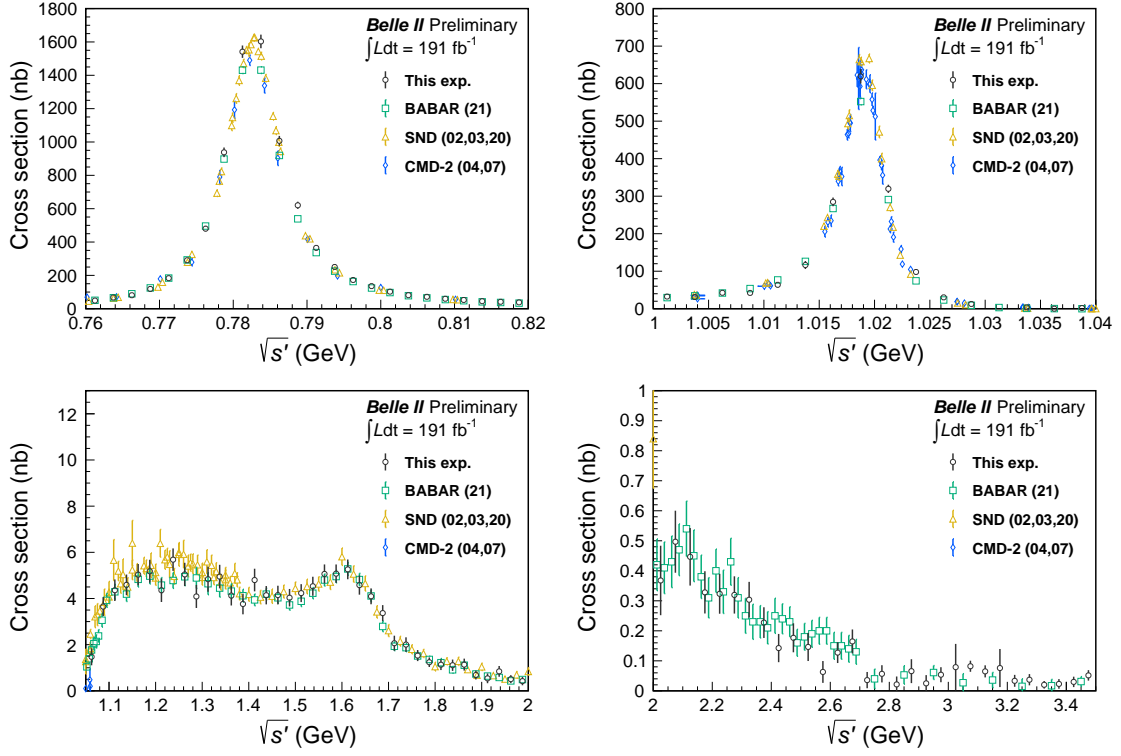


Figure 1: Observed $e^+e^- \rightarrow \pi^+\pi^-\pi^0$ cross section as a function of energy compared with previous results. Each panel covers a different energy range. Circles with error bars are the Belle II results, squares are the BABAR results [16], triangles are the SND results [17–19], and diamonds are the CMD-2 results [20, 21].

88 The contribution to the leading order HVP term in a_μ is given by

$$a_\mu^{\text{LO,HVP}} = \frac{\alpha}{3\pi^2} \int_{m_\pi^2}^{\infty} \frac{K(s)}{s} \frac{\sigma(e^+e^- \rightarrow \text{hadrons})}{4\pi\alpha^2/3s} ds, \quad (1)$$

89 where α is the fine-structure constant, $K(s)$ is the QED kernel function, and $\sigma(e^+e^- \rightarrow \text{hadrons})$
90 is the hadronic cross section [4]. The contribution obtained from the 3π cross section in the range
91 0.62–1.8 GeV measured by Belle II is

$$a_\mu^{3\pi} = (48.91 \pm 0.23 \pm 1.07) \times 10^{-10}.$$

92 This value is 6.5% larger than the global fit result [15] corresponding to 2.5 standard deviations.
93 This difference of 3×10^{-10} corresponds to a reduction of about 10% of the current discrepancy of
94 25×10^{-10} between the direct measurement of $g - 2$ and the SM prediction.

95 Acknowledgement

96 This work was supported by Japan Society for the Promotion of Science (JSPS) Research Fel-
97 lowship for Young Scientists-DC and JSPS KAKENHI Grant Numbers JP19J21763, JP18H05226,
98 22K21347, and JP23H05433.

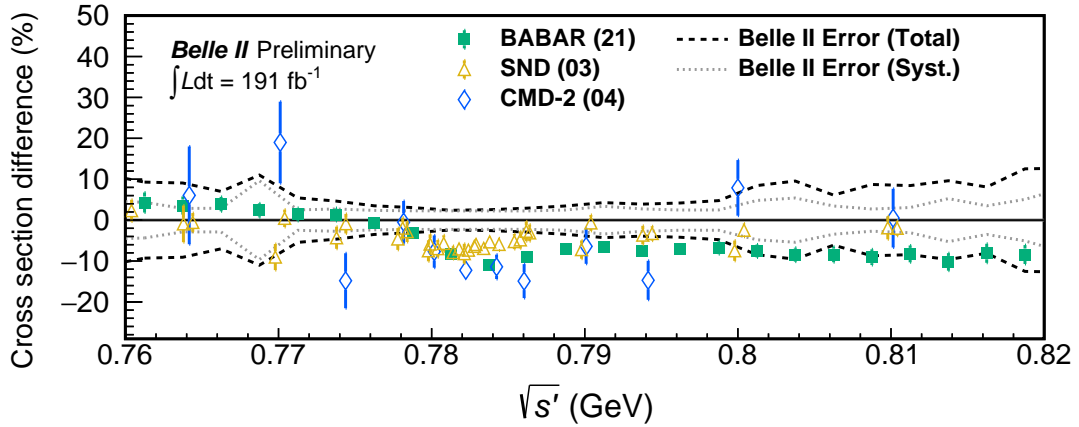


Figure 2: Differences between $e^+e^- \rightarrow \pi^+\pi^-\pi^0$ cross-section results from previous measurements and results of Belle II, as functions of energy (markers with error bars). Belle II results are taken as the reference at zero, with dashed (dotted) lines corresponding to the total (systematic) uncertainties. Squares are the BABAR results [16], triangles are the SND results [18], and diamonds are the CMD-2 results [20].

99 References

- 100 [1] MUON G-2 COLLABORATION collaboration, *Final Report of the Muon E821 Anomalous*
 101 *Magnetic Moment Measurement at BNL*, *Phys. Rev. D* **73** (2006) 072003
 102 [[hep-ex/0602035](#)].
- 103 [2] MUON G-2 COLLABORATION collaboration, *Measurement of the Positive Muon Anomalous*
 104 *Magnetic Moment to 0.46 ppm*, *Phys. Rev. Lett.* **126** (2021) 141801 [[2104.03281](#)].
- 105 [3] MUON G-2 COLLABORATION collaboration, *Measurement of the Positive Muon Anomalous*
 106 *Magnetic Moment to 0.20 ppm*, *Phys. Rev. Lett.* **131** (2023) 161802 [[2308.06230](#)].
- 107 [4] T. Aoyama *et al.*, *The anomalous magnetic moment of the muon in the Standard Model*, *Phys.*
 108 *Rept.* **887** (2020) 1 [[2006.04822](#)].
- 109 [5] Sz. Borsanyi *et al.*, *Leading hadronic contribution to the muon magnetic moment from lattice*
 110 *QCD*, *Nature* **593** (2021) 51 [[2002.12347](#)].
- 111 [6] M. Cè *et al.*, *Window observable for the hadronic vacuum polarization contribution to the*
 112 *muon g-2 from lattice QCD*, *Phys. Rev. D* **106** (2022) 114502 [[2206.06582](#)].
- 113 [7] EXTENDED TWISTED MASS COLLABORATION collaboration, *Lattice calculation of the short*
 114 *and intermediate time-distance hadronic vacuum polarization contributions to the muon*
 115 *magnetic moment using twisted-mass fermions*, *Phys. Rev. D* **107** (2023) 074506
 116 [[2206.15084](#)].
- 117 [8] RBC AND UKQCD COLLABORATIONS collaboration, *Update of Euclidean windows of the*
 118 *hadronic vacuum polarization*, *Phys. Rev. D* **108** (2023) 054507 [[2301.08696](#)].

- 119 [9] CMD-3 COLLABORATION collaboration, *Measurement of the Pion Form Factor with CMD-3*
120 *Detector and its Implication to the Hadronic Contribution to Muon ($g-2$)*, *Phys. Rev. Lett.*
121 **132** (2024) 231903 [2309.12910].
- 122 [10] SUPERKEKB collaboration, *The SuperKEKB Collider*, *Nucl. Instrum. Meth. A* **907** (2018)
123 188 [1809.01958].
- 124 [11] BELLE II COLLABORATION collaboration, *Belle II technical design report*, 1011.0352.
- 125 [12] B. Malaescu, *An Iterative, Dynamically Stabilized(IDS) Method of Data Unfolding*, in
126 *PHYSTAT 2011*, pp. 271–275, 2011, DOI [1106.3107].
- 127 [13] BELLE II COLLABORATION collaboration, *Measurement of the integrated luminosity of the*
128 *Phase 2 data of the Belle II experiment*, *Chin. Phys. C* **44** (2020) 021001 [1910.05365].
- 129 [14] BABAR COLLABORATION collaboration, *Measurement of additional radiation in the*
130 *initial-state-radiation processes $e^+e^- \rightarrow \mu^+\mu^-\gamma$ and $e^+e^- \rightarrow \pi^+\pi^-\gamma$ at BABAR*, *Phys. Rev.*
131 *D* **108** (2023) L111103 [2308.05233].
- 132 [15] M. Hoferichter, B.-L. Hoid, B. Kubis and D. Schuh, *Isospin-breaking effects in the three-pion*
133 *contribution to hadronic vacuum polarization*, *JHEP* **08** (2023) 208 [2307.02546].
- 134 [16] BABAR COLLABORATION collaboration, *Study of the process $e^+e^- \rightarrow \pi^+\pi^-\pi^0$ using initial*
135 *state radiation with BABAR*, *Phys. Rev. D* **104** (2021) 112003 [2110.00520].
- 136 [17] M. N. Achasov *et al.*, *Study of the process $e^+e^- \rightarrow \pi^+\pi^-\pi^0$ in the energy region \sqrt{s} from*
137 *0.98-GeV to 1.38-GeV*, *Phys. Rev. D* **66** (2002) 032001 [hep-ex/0201040].
- 138 [18] M. N. Achasov *et al.*, *Study of the process $e^+e^- \rightarrow \pi^+\pi^-\pi^0$ in the energy region \sqrt{s} below*
139 *0.98-GeV*, *Phys. Rev. D* **68** (2003) 052006 [hep-ex/0305049].
- 140 [19] V. M. Aul'chenko *et al.*, *Study of the $e^+e^- \rightarrow \pi^+\pi^-\pi^0$ process in the energy range 1.05–2.00*
141 *GeV*, *J. Exp. Theor. Phys.* **121** (2015) 27.
- 142 [20] CMD-2 COLLABORATION collaboration, *Reanalysis of hadronic cross-section measurements*
143 *at CMD-2*, *Phys. Lett. B* **578** (2004) 285 [hep-ex/0308008].
- 144 [21] R. R. Akhmetshin *et al.*, *Study of $\phi \rightarrow \pi^+\pi^-\pi^0$ with CMD-2 detector*, *Phys. Lett. B* **642**
145 (2006) 203.